



Cardiovascular Predictive Value and Genetic Basis of Ventricular Repolarization Dynamics

BACKGROUND: Early prediction of cardiovascular risk in the general population remains an important issue. The T-wave morphology restitution (TMR), an ECG marker quantifying ventricular repolarization dynamics, is strongly associated with cardiovascular mortality in patients with heart failure. Our aim was to evaluate the cardiovascular prognostic value of TMR in a UK middle-aged population and identify any genetic contribution.

METHODS: We analyzed ECG recordings from 55 222 individuals from a UK middle-aged population undergoing an exercise stress test in UK Biobank (UKB). TMR was used to measure ventricular repolarization dynamics, exposed in this cohort by exercise (TMR during exercise, TMR^{ex}) and recovery from exercise (TMR during recovery, TMR^{rec}). The primary end point was cardiovascular events; secondary end points were all-cause mortality, ventricular arrhythmias, and atrial fibrillation with median follow-up of 7 years. Genome-wide association studies for TMR^{ex} and TMR^{rec} were performed, and genetic risk scores were derived and tested for association in independent samples from the full UKB cohort (N=360 631).

RESULTS: A total of 1743 (3.2%) individuals in UKB who underwent the exercise stress test had a cardiovascular event, and TMR^{rec} was significantly associated with cardiovascular events (hazard ratio, 1.11; $P=5\times 10^{-7}$), independent of clinical variables and other ECG markers. TMR^{rec} was also associated with all-cause mortality (hazard ratio, 1.10) and ventricular arrhythmias (hazard ratio, 1.16). We identified 12 genetic loci in total for TMR^{ex} and TMR^{rec}, of which 9 are associated with another ECG marker. Individuals in the top 20% of the TMR^{rec} genetic risk score were significantly more likely to have a cardiovascular event in the full UKB cohort (18 997, 5.3%) than individuals in the bottom 20% (hazard ratio, 1.07; $P=6\times 10^{-3}$).

CONCLUSIONS: TMR and TMR genetic risk scores are significantly associated with cardiovascular risk in a UK middle-aged population, supporting the hypothesis that increased spatio-temporal heterogeneity of ventricular repolarization is a substrate for cardiovascular risk and the validity of TMR as a cardiovascular risk predictor.

VISUAL OVERVIEW: A [visual overview](#) is available for this article.

Julia Ramírez, PhD
Stefan van Duijvenboden, PhD
Nay Aung, MD, PhD
Pablo Laguna, PhD
Esther Pueyo, PhD
Andrew Tinker, MD, PhD*
Pier D. Lambiase, MD, PhD*
Michele Orini, PhD*
Patricia B. Munroe, PhD*

*Drs Tinker, Lambiase, Orini, and Munroe contributed equally as joint supervisors.

Key Words: exercise ■ genetic analyses ■ genetic risk score ■ middle aged ■ risk ■ T-wave morphology

© 2019 The Authors. *Circulation: Arrhythmia and Electrophysiology* is published on behalf of the American Heart Association, Inc., by Wolters Kluwer Health, Inc. This is an open access article under the terms of the [Creative Commons Attribution License](#), which permits use, distribution, and reproduction in any medium, provided that the original work is properly cited.

<https://www.ahajournals.org/journal/circep>



WHAT IS KNOWN?

- The T-wave morphology restitution (TMR) is a recently proposed ECG marker that quantifies the rate of variation of the T-wave morphology with heart rate.
- TMR is a strong predictor of sudden cardiac death in chronic heart failure patients.

WHAT THE STUDY ADDS?

- TMR at 1-minute recovery from exercise (TMR during recovery) was associated with cardiovascular risk (hazard ratio, 1.11; $P=5\times 10^{-7}$), all-cause mortality (hazard ratio, 1.10), and ventricular arrhythmic risk (hazard ratio 1.16) independent of clinical variables, resting corrected QT interval, and resting and recovery heart rate from an analysis of 60 000 individuals from a UK middle-aged population participating in an exercise stress test.
- Genetic loci for TMR during exercise and TMR during recovery were identified, of which 9 had been previously associated with other ECG markers. Individuals having a cardiovascular event in a $\approx 500\,000$ cohort had a higher genetic risk score for TMR during recovery than unaffected individuals.
- We demonstrate that TMR is a heritable risk marker for cardiovascular risk in a UK middle-aged population.

Cardiovascular mortality is the main cause of death in the general population,¹ and it accounts for 31% of all deaths worldwide, with its estimated cost expected to be \$1044 billion by 2030. Despite technological advances, prediction remains a critically important challenge.

The QT interval is the most recognized ECG index and reflects the duration of ventricular depolarization and repolarization. However, increasing evidence suggests that dispersion of repolarization and, in particular, its variations with heart rate, is a stronger marker for cardiovascular risk than the total duration of repolarization.^{2,3} The T-wave morphology restitution (TMR)⁴ is a recently proposed ECG marker that quantifies the rate of variation of the T-wave morphology with heart rate. This marker has shown to be a strong predictor of sudden cardiac death in chronic heart failure patients.^{4,5} However, its performance as a potential cardiovascular risk marker in the general population has not been evaluated. Furthermore, the biological mechanisms underlying TMR are not known.

ECG markers are heritable⁶ and statistical genetic methods are available to estimate the cumulative contribution of genetic factors to cardiovascular events via genetic risk scores (GRSs).⁷ We hypothesize that the interaction between repolarization dynamics and cardiovascular risk has a genetic component and that TMR can be used to capture it.

Our primary objective was to validate the prognostic significance of TMR in a dataset of 55 222 individuals where exercise and recovery from exercise were used to expose spatio-temporal heterogeneity of ventricular repolarization. Our secondary objectives were to perform genome-wide association studies (GWASs) to identify single-nucleotide variants (SNVs) determining the genetic contribution of TMR and to develop GRSs to evaluate their association with cardiovascular events in an independent population of 360 631 individuals.

METHODS

Anonymized data and materials have been returned to UK Biobank (UKB) and can be accessed per request.

Study Population, Follow-Up, and End Points

UKB is a prospective study of 488 377 individuals (FULL-UKB cohort), comprising relatively even numbers of men and women aged 40 to 69 years old at recruitment (2006–2008). A total of 95 216 individuals were invited for an exercise test using a stationary bicycle in conjunction with a 1-lead ECG device (Methods in the [Data Supplement](#)). Complete ECG recordings from 58 839 individuals, who were considered fit to perform the exercise stress test (EST), were available (EST in UKB [EST-UKB] cohort; Figure 1). Individuals were excluded if they had existing medical conditions known to affect heart rate, if they had experienced a previous cardiovascular event (matching the codes from Table I in the [Data Supplement](#)), if they were on heart rate altering medications, had been diagnosed with bundle branch block, if the ECG had poor quality, or there was no heart rate change during the exercise test (Methods in the [Data Supplement](#)). This led to $N=55\,222$ individuals included in the analyses. The UKB study has approval from the North West Multi-Centre Research Ethics Committee, and all participants provided informed consent.⁸

The primary end point of this study was cardiovascular events, defined as cardiovascular mortality or admission to hospital with a cardiovascular diagnosis. The exact *International Classification of Diseases, Tenth Revision* codes used to define cardiovascular events are presented in Table I in the [Data Supplement](#). The secondary end points were all-cause mortality (excluding external causes), ventricular arrhythmic events (defined as arrhythmic mortality or admission to hospital with an arrhythmic diagnosis), and atrial fibrillation. Details on cause and date of death and diagnoses are available in the Methods in the [Data Supplement](#). Follow-up was from the study inclusion date until March 31, 2017.

Derivation of TMR During Exercise and TMR During Recovery

The bicycle ergometer exercise test followed a standardized protocol: 15 s resting period, 2 minutes of constant load, 4 minutes of exercise during which the workload was gradually increased, and a 1-minute recovery period without pedaling (Figure 2A). Details of the preprocessing of

the ECG recordings are available in the Methods in the [Data Supplement](#). Automatic quantification of TMR during exercise (TMR^{ex}) and recovery (TMR^{rec}; shown in Figure 2) was performed on every ECG recording in 3 steps:

1. Derivation of average T waves: signal averaging of all available heartbeats within a 15 s window at rest, peak exercise, and recovery was used to reduce noise (Figure 2B). The onset, peak, and offset timings of the waveforms were located using bespoke software.^{9,10} Average T waves at rest, peak exercise, and recovery were selected using the T onset and T offset timings and were further low-pass filtered at 20 Hz.
2. T-wave morphology differences quantification: using a previously published algorithm based on time warping,¹¹ we derived the marker dw^{ex} , representing the average temporal stretching necessary to align each point of the average T wave at rest to the average T wave at peak exercise.¹¹ Figure 2C shows an example where 2 T waves have similar morphology and small dw^{ex} . Similarly, the marker dw^{rec} represents the average temporal stretching necessary to align each point of the average T wave at peak exercise and the average T wave at recovery. Figure 2C shows that the morphological difference between the 2 T waves has increased along with dw^{rec} .
3. TMR calculations: TMR^{ex} and TMR^{rec} were calculated by dividing dw^{ex} and dw^{rec} by the change in the RR interval (inverse of heart rate) during exercise, ΔRR^{ex} , and during recovery, ΔRR^{rec} , respectively, and represent the T-wave morphological change per RR increment during exercise and recovery, respectively.⁴

Computation of Other ECG markers

The QT interval and QRS duration were measured as the interval between the QRS-onset and the T-wave end, and between the QRS-onset and the QRS-offset, respectively, from the averaged heartbeat at rest. Then, we corrected the QT interval using Bazett formula.¹² We additionally derived the marker T-wave inversion, which indicated a change in the polarity of the T waves between resting and exercise stages¹³ (Methods in the [Data Supplement](#)).

Statistical Analyses

The 2-tailed Mann-Whitney and Fisher exact tests were used for univariate comparison of quantitative and categorical data, respectively. Correlation was evaluated with Spearman correlation coefficient. Receiver operator curves were derived using the pROC package¹⁴ from R and C-indices were calculated for each marker. We estimated the optimal cutoff values for TMR^{ex} and TMR^{rec} in a training set (N=27612) from the EST-UKB cohort (Methods in the [Data Supplement](#)) by means of log-rank statistics optimization with the aim of maximizing the predictive value. Kaplan-Meier curves were derived using the optimal cutoff values in the test set (N=27610), with a comparison of cumulative events performed by using log-rank tests.

Univariate and multivariate Cox regression analyses were performed to determine the predictive value of the risk markers. The proportional hazard assumptions were checked when applying these analyses. Continuous variables were

standardized to a mean of 0 and SD of 1 to allow for comparisons in the Cox models. Only the variables with a significant association with the end point in univariate analysis were included in the multivariate model. Individuals who died from causes not included in the primary end point were censored at the time of death. A value of $P < 0.05$ was considered statistically significant. Statistical analyses were performed using R version 3.5.1.

Heritability and GWASs

Inverse-normal transformation of TMR^{ex} and TMR^{rec} was performed as the distributions were skewed and did not approximate a normal distribution (Figure 1 in the [Data Supplement](#)). Heritability was estimated using a variance components method (BOLT-REML).¹⁵ GWAS for TMR^{ex} and TMR^{rec} were performed in a discovery (N=29393) and replication (N=22382) datasets separately using a linear mixed model method (BOLT-LMM).¹⁶ The TMR^{ex} model included the following covariates: sex, age, body mass index (BMI), resting RR, ΔRR^{ex} and a binary indicator variable for the genotyping array (UKB versus UK BiLEVE). The TMR^{rec} model included covariates sex, age, BMI, recovery RR, ΔRR^{rec} and the genotyping array. After careful review of significant ($P < 1 \times 10^{-6}$) SNVs from the discovery GWASs, 6 variants for TMR^{ex} and 7 variants for TMR^{rec} were taken forward into replication. Replication was confirmed if the SNVs remained significant (with Bonferroni correction) and with concordant direction of effects to the discovery analyses. A full dataset GWAS for both TMR^{ex} and TMR^{rec} was conducted and additional loci reaching genome-wide significance ($P < 5 \times 10^{-8}$) were reported. Since TMR^{ex} and TMR^{rec} were genetically correlated ($\rho = 0.58$), multitrait analysis of GWAS¹⁷ was used to leverage additional loci discovery. Detailed information can be found in Methods in the [Data Supplement](#).

To examine if there were independent secondary SNVs at TMR loci, we applied genome-wide complex trait analysis¹⁸ for all reported loci from the full dataset GWAS. The percent variance of TMR^{ex} and TMR^{rec} explained by the identified loci was calculated with standard methods, detailed in the Methods in the [Data Supplement](#). Bioinformatics analyses were performed to annotate SNVs and identify candidate genes, including Variant Effect Predictor,¹⁹ GTEx (the Genotype-Tissue Expression project), and long-range chromatin interaction data.²⁰ We used PhenoScanner,²¹ GWAS catalog (<https://www.ebi.ac.uk/gwas/>), and UKBiobank ICD PheWeb (<http://pheweb.sph.umich.edu/SAIGE-UKB/>) to determine SNV and gene associations with other traits. Pathway analyses were performed using g:profiler.²² Further description of bioinformatics analyses can be found in the Methods in the [Data Supplement](#). We downloaded the summary statistics for atrial fibrillation²³ to calculate its genetic correlation with TMR^{ex} and TMR^{rec} using LD score regression.²⁴

Genetic Risk Score Analyses

We used PRSice v2²⁵ to construct the GRS for TMR^{ex} and TMR^{rec} using the effect sizes from the full-cohort GWASs (EST-UKB) and performed prediction for the primary end point in the full UKB cohort (FULL-UKB) dataset (after exclusions, Figure II and Methods in the [Data Supplement](#)). We

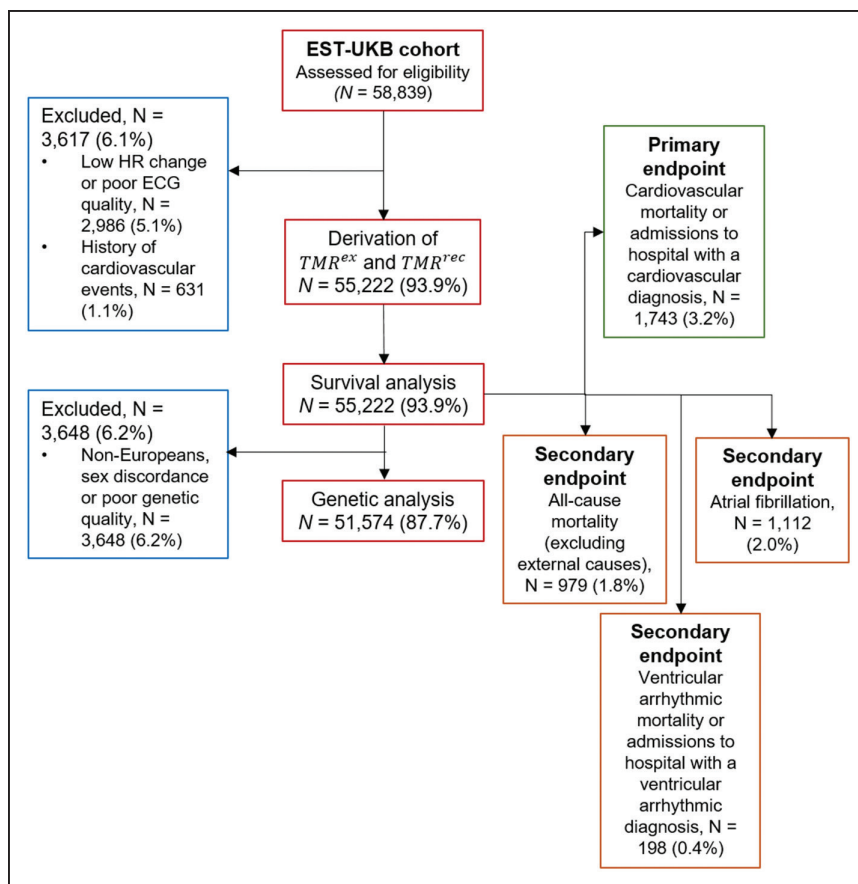


Figure 1. Flow diagram of analyses in the exercise stress test (EST; EST in UK Biobank [EST-UKB]) population. HR indicates heart rate; TMR, T-wave morphology restitution; TMR^{ex}, TMR during exercise; and TMR^{rec}, TMR during recovery.

first removed individuals included in the GWASs (EST-UKB) and their relatives, then removed all individuals with a previous history of cardiovascular events and non-Europeans. The GRSs were standardized to have a mean of 0 and an SD of 1. Their association with the study end points was tested in the FULL-UKB cohort (after exclusions, Figure II in the [Data Supplement](#)) using Mann-Whitney and Univariate Cox regression analyses.

RESULTS

Predictive Value of TMR in a UK Middle-Aged Population

The EST-UKB population consisted of 55222 individuals (25669 males, 29553 females) aged 40 to 73 years (mean 57 ± 8 years) after exclusions. The demographic characteristics of this population are shown in Table II in the [Data Supplement](#). During the follow-up, 1743 (3.2%) individuals had a cardiovascular event. The distributions of TMR^{ex} and TMR^{rec} are shown in Figure I in the [Data Supplement](#).

Age, BMI, TMR^{rec} ($P < 2 \times 10^{-16}$ for all), TMR^{ex} ($P = 3 \times 10^{-8}$) and resting heart rate ($P = 3 \times 10^{-4}$) were significantly higher in the cardiovascular events group than in the event-free group, whereas heart rate response to exercise and recovery were lower

($P < 2 \times 10^{-16}$ for both). Also, there were more males, diabetics, hypertensives (stage 1 [130 mm Hg \leq systolic blood pressure < 140 mm Hg or 85 mm Hg \leq diastolic blood pressure < 90 mm Hg] and stage 2 [systolic blood pressure ≥ 140 mm Hg or diastolic blood pressure ≥ 90 mm Hg]), individuals with high cholesterol levels ($P < 2 \times 10^{-16}$ for all), smokers ($P = 1 \times 10^{-13}$), diagnosed with chronic kidney disease ($P = 5 \times 10^{-2}$), or with T-wave inversions ($P = 9 \times 10^{-3}$). QRS duration was not significantly different in individuals with and without cardiovascular events and thus was not included in the survival analyses (Table III and Figure III in the [Data Supplement](#)). Spearman correlation coefficient between TMR^{ex} and TMR^{rec} was 0.484; lower correlations were found between them and covariates (Table IV in the [Data Supplement](#)).

Individuals in the TMR^{ex} ≥ 0.082 group (stratified according to the optimal cutoff value—Figure IV in the [Data Supplement](#)) had 1.65 fold risk (95% CI, 1.38–1.98) of having a cardiovascular event than those in the TMR^{ex} < 0.082 group ($P < 10^{-3}$; Figure 3A). Similarly, individuals in the TMR^{rec} ≥ 0.115 group (Figure V in the [Data Supplement](#)) had 1.71 fold risk (95% CI, 1.43–2.05) of having a cardiovascular event than those in the TMR^{rec} < 0.115 groups ($P < 10^{-3}$; Figure 3B).

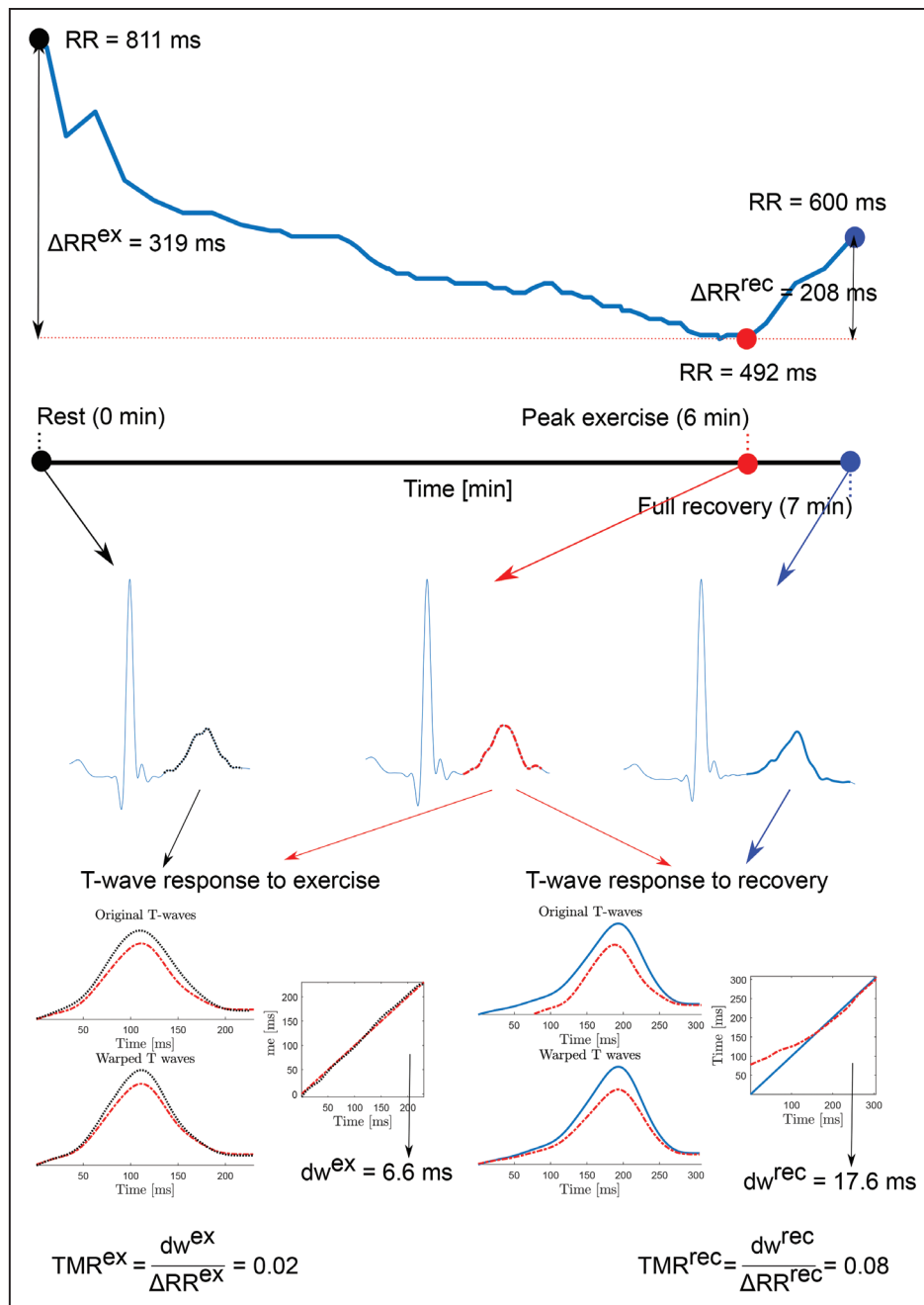


Figure 2. Assessment of T-wave morphology restitution (TMR).

A, Illustration of the RR profile during the exercise stress test. **B**, Three averaged heartbeats are derived at rest (black), peak exercise (red) and 50 s after peak exercise (full recovery, blue), respectively. **C**, TMR during exercise (TMR^{ex}) and TMR during recovery (TMR^{rec}) are derived by quantifying the morphological change between the T waves at rest (black T wave) and at peak exercise (red T wave), and between the T waves at peak exercise and full recovery (blue T wave), respectively, normalized by the corresponding RR change. ΔRR^{ex} indicates change in RR interval during exercise; and ΔRR^{rec} , change in RR interval during recovery.

To compare the hazard ratios (HRs) of TMR^{ex} and TMR^{rec} with those from other continuous markers, independently from cutoff thresholds, we included the continuous TMR^{ex} and TMR^{rec} markers into a multivariate Cox regression model. The following variables remained significantly associated with cardiovascular events (HR [95% CI] reported): chronic kidney disease (2.85 [1.07–7.62]), sex (2.82 [2.52–3.15]), T-wave inversion (2.21 [1.10–4.45]), age (1.73 [1.63–1.84]),

diabetes mellitus (1.56 [1.32–1.84]), hypertension stage 2 (1.32 [1.15–1.51]), hypertension stage 1 (1.19 [1.02–1.39]), BMI (1.18 [1.13–1.25]), corrected QT interval (1.11 [1.06–1.17]), and TMR^{rec} (1.11 [1.07–1.16]; Table 1). Among ECG markers, resting heart rate, heart rate responses to exercise and recovery, and TMR^{ex} were no longer significant. Among all cardiovascular events, 81.7% were related to ischemic heart disease. TMR^{rec} was independently associated

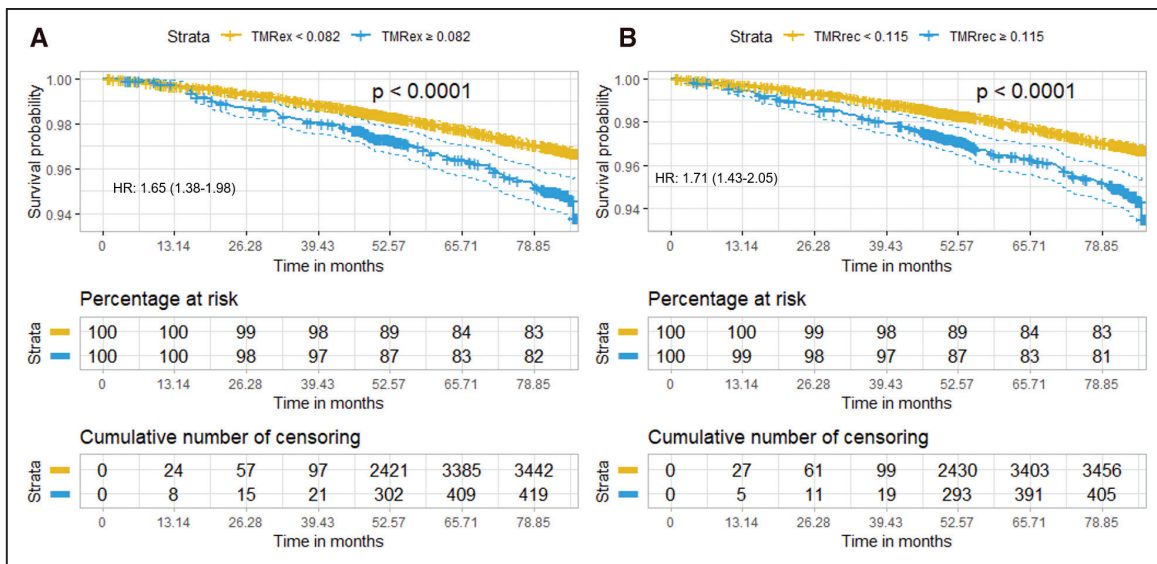


Figure 3. Kaplan-Meier survival curves. Cumulative survival rates of individuals stratified by T-wave morphology restitution (TMR) during exercise (TMR^{ex}) of ≥0.082 (A) and by TMR during recovery (TMR^{rec}) of ≥0.115 (B). Dashed lines indicate the 95% confidence levels. HR indicates hazard ratio.

with both ischemic (HR [95% CI] of 1.08 [1.03–1.13]) and nonischemic (HR [95% CI] of 1.20 [1.11–1.30]) causes (Tables VA and VB in the [Data Supplement](#)). The assumption of proportional hazards was supported for all covariates.

For the secondary end points, there were 979 (1.8%) cases of all-cause mortality, 198 (0.4%) who had a ventricular arrhythmic event, and 1112 (2.0%) who had atrial fibrillation (Table II in the [Data Supplement](#)). In multivariate Cox analysis, TMR^{rec} remained significantly associated

Table 1. Association With Cardiovascular Risk

	Univariate		Multivariate	
	HR (95% CI)	P Value	HR (95% CI)	P Value
Clinical variables				
Age (per 1 SD)	1.88 (1.78–2.00)	<2×10 ⁻¹⁶ *	1.73 (1.63–1.84)	<2×10 ⁻¹⁶ *
Sex (male)	3.01 (2.70–3.35)	<2×10 ⁻¹⁶ *	2.82 (2.52–3.15)	<2×10 ⁻¹⁶ *
Diabetes mellitus (yes)	2.71 (2.31–3.19)	<2×10 ⁻¹⁶ *	1.56 (1.32–1.84)	2.20×10 ⁻⁷ *
High cholesterol (yes)	1.95 (1.72–2.20)	<2×10 ⁻¹⁶ *	1.10 (0.97–1.25)	1.60×10 ⁻¹
BMI (per 1 SD)	1.28 (1.23–1.34)	<2×10 ⁻¹⁶ *	1.18 (1.13–1.25)	3.00×10 ⁻¹¹ *
Hypertensive stage 1	1.72 (1.48–2.01)	4.10×10 ⁻¹² *	1.19 (1.02–1.39)	2.60×10 ⁻² *
Hypertensive stage 2	2.43 (2.14–2.76)	<2×10 ⁻¹⁶ *	1.32 (1.15–1.51)	4.70×10 ⁻⁵ *
Previous or current smoker (yes)	1.38 (1.25–1.53)	9.30×10 ⁻¹¹ *	1.10 (0.99–1.21)	8.60×10 ⁻²
CKD (yes)	3.62 (1.36–9.66)	1.00×10 ⁻² *	2.85 (1.07–7.62)	3.70×10 ⁻² *
ECG variables				
Resting heart rate (per 1 SD)	1.10 (1.05–1.15)	5.70×10 ⁻⁵ *	0.97 (0.91–1.03)	2.90×10 ⁻¹
Heart rate response to exercise (per 1 SD)	0.70 (0.66–0.74)	<2×10 ⁻¹⁶ *	1.02 (0.94–1.10)	6.70×10 ⁻¹
Heart rate response to recovery (per 1 SD)	0.74 (0.71–0.76)	<2×10 ⁻¹⁶ *	0.96 (0.90–1.03)	2.50×10 ⁻¹
Corrected QT (per 1 SD)	1.15 (1.10–1.20)	4.00×10 ⁻¹⁰ *	1.11 (1.06–1.17)	5.40×10 ⁻⁵ *
T-wave inversion (yes)	2.80 (1.40–5.60)	3.70×10 ⁻³ *	2.21 (1.10–4.45)	2.70×10 ⁻² *
TMR during exercise (per 1 SD)	1.17 (1.12–1.22)	6.10×10 ⁻¹⁵ *	1.03 (0.98–1.08)	2.50×10 ⁻¹
TMR during recovery (per 1 SD)	1.23 (1.19–1.28)	<2×10 ⁻¹⁶ *	1.11 (1.07–1.16)	4.90×10 ⁻⁷ *

Hypertensive stage 1 defined as 130 mm Hg ≤ SBP <140 mm Hg or 85 mm Hg ≤ DBP <90 mm Hg. Hypertensive stage 2 defined as SBP ≥140 mm Hg or DBP ≥90 mm Hg. Reference Hypertension group is Hypertensive stage 0, defined as SBP <130 mm Hg and DBP <85 mm Hg. BMI indicates body mass index; CKD, chronic kidney disease; DBP, diastolic blood pressure; HR, hazard ratio; SBP, systolic blood pressure; and TMR, T-wave morphology restitution.

*Indicates statistically significant.

Table 2. Loci Associated With TMR During Exercise

Locus	SNV	CHR	BP	EA	EAF	Discovery			Replication			Combined					
						P Value	N	β	SE	P Value	N	β	SE	P Value	N	β	SE
RNF207§	rs709208	1	6272137	A	0.679	2.60×10 ⁻⁷	27 939	-0.042	0.008	1.60×10 ⁻⁵	20 769	-0.040	0.009	1.80×10 ⁻¹¹	49 203	-0.041	0.006
NOS1AP*†	rs12143842	1	162033890	C	0.750	1.20×10 ⁻⁴	29 393	-0.033	0.008	3.40×10 ⁻³	21 850	-0.029	0.010	6.60×10 ⁻⁷	51 764	-0.032	0.006
SCN5A-SCN10A*‡	rs7428232	3	38778618	T	0.416	5.20×10 ⁻⁶	29 352	-0.034	0.007	1.80×10 ⁻⁴	21 820	-0.032	0.008	3.70×10 ⁻⁹	51 692	-0.033	0.006
PREP	rs4478445	6	105786660	C	0.943	2.50×10 ⁻⁵	28 913	-0.067	0.016	7.40×10 ⁻³	21 493	-0.049	0.018	8.00×10 ⁻⁷	50 919	-0.059	0.012
KCNH2	rs2072412	7	150647970	C	0.729	1.80×10 ⁻⁶	28 975	0.040	0.008	4.10×10 ⁻⁷	21 539	0.048	0.010	2.10×10 ⁻¹¹	51 028	0.042	0.006
KCNQ1*§	rs2074238	11	2484803	T	0.088	1.10×10 ⁻⁸	29 393	-0.073	0.013	1.20×10 ⁻³	21 850	-0.048	0.015	1.20×10 ⁻¹	51 764	-0.062	0.010
SOX5*§	rs7307613	12	24595192	C	0.505	1.80×10 ⁻⁷	29 359	0.038	0.007	3.50×10 ⁻⁶	21 825	0.039	0.008	2.80×10 ⁻¹²	51 704	0.039	0.006
KCNJ2§	17:68493468_GA_G	17	68493468	GA	0.674	7.60×10 ⁻⁷	29 318	0.039	0.008	3.70×10 ⁻⁷	21 794	0.046	0.009	2.90×10 ⁻¹³	51 632	0.043	0.006

The locus name indicates the gene that is in the closest proximity to the most associated SNV. BP indicates position, based on human genome build 19; CHR, chromosome; EA, effect allele; EAF, effect allele frequency from discovery data; LD, linkage disequilibrium; MTAG, multitrait analysis of genome-wide association study; N, number of participants; SNV, single-nucleotide variation; and TMR, T-wave morphology restitution.

*SNV is the same or in high LD ($r^2>0.8$) with an SNV associated with the other index.
 †Identified with MTAG.
 ‡Has a secondary signal.
 §Replicated SNVs.

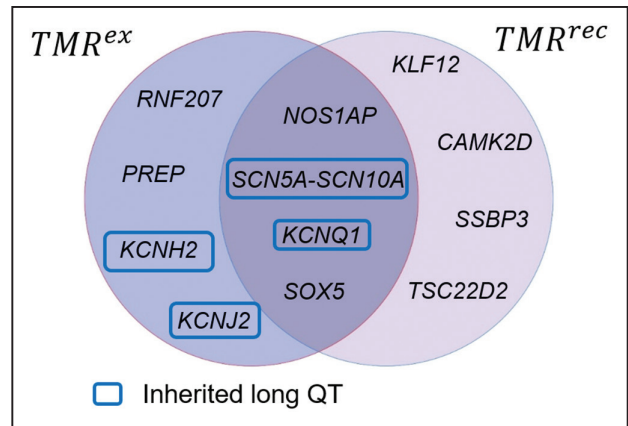


Figure 4. Overlap of loci for T-wave morphology restitution (TMR) during exercise (TMR^{ex}) and TMR during recovery (TMR^{rec}). The loci names indicate the coding gene that is in the closest proximity to the most associated single-nucleotide variation.

with all-cause mortality (HR [95% CI] of 1.10 [1.04–1.17]) independently of age, sex, smoke, diabetes mellitus, resting heart rate, heart rate response to recovery, and heart rate response to exercise (Table VI in the [Data Supplement](#)). TMR^{rec} also remained significantly associated with ventricular arrhythmic events (HR [95% CI] of 1.16 [1.03–1.30]) independently of sex, age, and heart rate response to recovery (Table VII in the [Data Supplement](#)). Finally, TMR^{rec} was not independently associated with atrial fibrillation (Table VIII in the [Data Supplement](#)).

Twelve Genetic Loci Are Associated With TMR

A total of 51 574 subjects were taken forward for genetic analyses after applying genetic quality control and excluding individuals of non-European ancestry (Figure 1). The heritability estimations of TMR^{ex} and TMR^{rec} were 3.5% and 4.9%, respectively, and their phenotypic correlation was 0.43.

In the discovery cohort GWAS (Methods), 1 genome-wide significant ($P \leq 5 \times 10^{-8}$) locus was found for TMR^{ex}, and 3 for TMR^{rec} (Table IX in the [Data Supplement](#)). Four SNVs for TMR^{ex} and 3 for TMR^{rec} formally replicated in the independent validation cohort (Tables 2 and 3). In the full dataset analysis, 2 additional SNVs reached genome-wide significance for TMR^{ex} and 4 SNVs for TMR^{rec}, respectively, all with concordant directions of effect (Tables 2 and 3). Manhattan plots for the full dataset are shown in Figure VI in the [Data Supplement](#). Visual inspection of the corresponding QQ plots from the discovery and full dataset GWASs did not show evidence of *P* value inflation or confounding (Figure VII in the [Data Supplement](#)). Analysis using multitrait analysis of GWAS¹⁷ (Methods) indicated 2 additional loci were significantly associated with TMR^{ex} and 1 for TMR^{rec} (Tables XA and XB in the [Data Supplement](#)). Sex-stratified analyses did not identify sex-specific loci for TMR^{ex}

Table 3. Loci Associated With TMR During Recovery

Locus	SNV	CHR	BP	EA	EAF	Discovery			Replication			Combined					
						P Value	N	β	SE	P Value	N	β	SE	P Value	N	β	SE
SSBP3	rs562408	1	54742618	A	0.430	6.20×10 ⁻⁶	28299	0.030	0.007	7.40×10 ⁻³	21091	0.020	0.008	3.70×10 ⁻⁸	49895	0.027	0.005
NOS1AP [§]	rs12143842	1	162033890	C	0.750	8.10×10 ⁻⁹	29013	-0.043	0.007	1.60×10 ⁻⁸	21623	-0.048	0.009	5.10×10 ⁻¹⁶	51153	-0.045	0.006
SCN5A-SCN10A**	rs7373065	3	38710315	T	0.019	2.00×10 ⁻⁶	26979	0.114	0.024	2.10×10 ⁻⁶	20107	0.132	0.028	1.60×10 ⁻¹¹	47566	0.122	0.018
TSC22D2	rs112717154	3	149943115	G	0.863	1.40×10 ⁻⁶	27857	-0.046	0.010	5.30×10 ⁻³	20762	-0.031	0.011	9.30×10 ⁻⁹	49115	-0.041	0.007
CAIMK2D	rs35408611	4	114423677	C	0.738	6.20×10 ⁻³	28362	-0.020	0.007	1.40×10 ⁻⁸	21138	-0.048	0.008	2.90×10 ⁻⁸	50006	-0.031	0.006
KCNQ1*§	rs2074238	11	2484803	T	0.088	1.40×10 ⁻³¹	29013	-0.131	0.011	4.20×10 ⁻³¹	21623	-0.152	0.013	1.20×10 ⁻⁵⁹	51153	-0.138	0.008
SOX5*§	rs1396206	12	24576859	A	0.482	3.10×10 ⁻¹³	28318	0.048	0.007	4.00×10 ⁻⁵	21105	0.031	0.007	1.30×10 ⁻¹⁶	49927	0.040	0.005
KLF12†	rs7992314	13	74509346	G	0.631	2.50×10 ⁻⁶	28908	-0.032	0.007	6.00×10 ⁻³	21545	-0.021	0.008	6.40×10 ⁻⁸	50968	-0.027	0.005

The locus name indicates the gene that is in the closest proximity to the most associated SNV. BP indicates position, based on human genome build 19; CHR, chromosome; EA, effect allele; EAF, effect allele frequency from discovery data; LD, linkage disequilibrium; MTAG, multitrait analysis of genome-wide association study; N, number of participants; SNV, single-nucleotide variation; and TMR, T-wave morphology restitution.

*SNV is the same or in high LD ($r^2>0.8$) with an SNV associated with the other index.

†Identified with MTAG.

#Has a secondary signal.

§Replicated SNVs.

or TMR^{rec}. Conditional analyses showed evidence for 2 secondary independent signals at the *SCN5A-SCN10A* locus, 1 for each trait (Tables 2 and 3).

In total, 12 loci were identified, 8 for each trait with SNVs at 4 loci associated with both markers (Figure 4). The lead SNVs at the shared loci at *NOS1AP*, *KCNQ1*, *SCN5A-SCN10A*, and *SOX5* were identical or in high linkage disequilibrium ($r^2>0.8$). The identified SNVs for TMR^{ex} explained 0.63% of its variance. Similarly, the 8 SNVs identified for TMR^{rec} explained 1.14% of its variance. This corresponds to 20% and 23% of the estimated heritability for each TMR marker, respectively.

Variants at 7 of the 12 TMR loci have previously been reported to be associated with resting QT (*RNF207*, *KCNH2*, *KCNJ2*, *NOS1AP*, *SCN5A-SCN10A*, *KCNQ1*, and *KLF12*). Regional plots are shown in Figure VIII in the [Data Supplement](#). Look-ups in PhenoScanner indicated 9 of the 12 SNVs have associations with other cardiovascular markers, including pulse rate, QT interval, PR interval, QRS duration, P-wave duration, cardiac arrhythmias, and heart function (Tables XIA and XIB in the [Data Supplement](#)).

None of the lead variants or their close proxies ($r^2>0.8$) were annotated as missense variants. Variants at 2 loci *NOS1AP* and *SSBP3* were associated with expression levels of nearby genes (*c1orf226* and *SSBP3*, respectively) in heart atrial appendage samples (Table XII in the [Data Supplement](#)). We found 11 potential target genes whose promoter regions form significant chromatin interactions at 9 TMR loci (Table XIII in the [Data Supplement](#)). Using this information and literature review, we derived a list of candidate genes at each locus (Table XIV in the [Data Supplement](#)).

Table XV in the [Data Supplement](#) shows a lookup of all candidate genes in the GWAS catalog and in UKBio-bank ICD PheWeb and indicate associations across different cardiovascular traits, including atrial fibrillation. Our LD Score regression analysis indicated there was no significant genetic correlation between TMR^{ex} or TMR^{rec} and atrial fibrillation. The top 3 biological pathways for TMR^{ex} were cardiac muscle cell action potential ($P=4\times 10^{-10}$), regulation of ventricular cardiac muscle cell membrane repolarization ($P=4.7\times 10^{-10}$), and ventricular cardiac muscle cell membrane repolarization ($P=1\times 10^{-9}$; Figure IX in the [Data Supplement](#)). The analyses for TMR^{rec} indicated similar pathways including cardiac muscle cell action potential ($P=6.6\times 10^{-8}$), regulation of cardiac muscle contraction ($P=1.2\times 10^{-7}$), and regulation of striated muscle contraction ($P=3\times 10^{-7}$, Figure X in the [Data Supplement](#)).

Predictive Value of GRSs for TMR

After excluding individuals from the EST-UKB cohort and applying the exclusion criteria defined in Methods, the FULL-UKB population consisted of 360631 healthy

individuals (160 793 men, 199 838 women) aged 40 to 73 years (mean 57 ± 8 years, Figure II and Table II in the [Data Supplement](#)). During the follow-up, 18 997 (5.3%) individuals had a cardiovascular event, and 12 081 (3.3%), 2040 (0.6%) and 14 517 (4.0%) were individuals of all-cause mortality, ventricular arrhythmic events, and atrial fibrillation, respectively.

The optimal GRS for TMR^{ex} was derived combining 3442 SNVs identified using a P value of 3.1×10^{-3} for thresholding (Figure XI in the [Data Supplement](#)). This GRS was not significantly different between individuals with a cardiovascular event and those without ($P=5.5 \times 10^{-2}$). The optimal GRS for TMR^{rec} was derived combining 3281 SNVs with a $P < 2.9 \times 10^{-3}$ (Figure XII in the [Data Supplement](#)). The TMR^{rec} GRS was significantly higher in individuals with a cardiovascular event than those that did not have an event ($P=1.5 \times 10^{-2}$). Univariate Cox analysis showed that individuals in the top 20% of the GRS for TMR^{rec} were significantly more likely to have a cardiovascular event than those in the bottom 20% (HR [95% CI] of 1.07 [1.02–1.12]; $P=5.9 \times 10^{-3}$). No significant associations were found with the secondary end points for the 2 GRSs.

DISCUSSION

TMR is a recently developed ECG marker to measure the rate of variation of the T-wave morphology due to heart rate changes. TMR is associated with spatio-temporal heterogeneity of ventricular repolarization,¹¹ exposed in this cohort by exercise and recovery from exercise. The main findings of this study are (1) TMR^{rec} is significantly associated with cardiovascular events, all-cause mortality, and ventricular arrhythmias in a UK middle-aged population and (2) the identified loci for TMR^{rec} show a significant association with cardiovascular events despite limited heritability.

TMR^{rec} was an independent predictor of cardiovascular risk, after adjustment for conventional predictors (age, sex, diabetes mellitus, BMI, smoking, chronic kidney disease, and hypertension) and other ECG markers, including heart rate, corrected QT interval, and T-wave inversions in a general UK middle-aged population (Table 1). In this population, the majority of cardiovascular events were related to ischemic heart disease, and TMR^{rec} was associated with cardiovascular events in both ischemic and nonischemic individuals (Tables VA and VB in the [Data Supplement](#)). Well-established predictors of cardiovascular risk, like resting heart rate,²⁶ chronotropic incompetence, or heart rate recovery,²⁷ did not remain significantly associated with cardiovascular events after adjustment for ECG markers of ventricular repolarization (corrected QT interval, T-wave inversion, and TMR^{rec}). This suggests that ventricular repolarization abnormalities may play a more impor-

tant role in creating a substrate for malignant cardiovascular events than heart rate markers in a UK middle-aged population. The QRS duration was not associated with cardiovascular events in our population; this may be explained by our cohort being a low-risk population, and we had excluded individuals with previous cardiovascular events. We suggest that future analyses should incorporate additional ECG indices with similar proven findings in individuals undergoing an EST.²⁸

In our previous work, TMR predicted sudden cardiac death in a population of 651 chronic heart failure patients.^{4,5} In that work, TMR, derived from 24-hour ambulatory Holter recordings, was the strongest sudden cardiac death predictor compared with other markers, including left ventricular ejection fraction, QRS duration, or T-wave alternans.⁴ Interestingly, although the prevalence of ventricular arrhythmic events in the current study is too small to infer any robust conclusions (0.4% in UKB-EST, compared with 8.4% in the published chronic heart failure study), our results seem to support an association of TMR with sudden cardiac death (Table VII in the [Data Supplement](#)). In this study, TMR^{rec} was not significantly associated with atrial fibrillation.

We observed the heritability of TMR^{ex} and TMR^{rec} to be 3.5% and 4.9%, respectively, in our data set, suggesting that the mechanisms underlying TMR are largely affected by environmental factors. Despite low heritability, we identified 12 loci associated with TMR^{ex} and TMR^{rec} , 4 of which were common to both markers (Figure 4). Genetic variations at 4 of the 8 loci identified for TMR^{ex} have previously been associated with long-QT syndrome and QT in the general population: *KCNH2*, *KCNJ2*, *SCN5A*, and *KCNQ1*,²⁹ all proven regulators of cardiac excitation through regulation of the action potential duration and cardiac repolarizing channels.³⁰ *KCNQ1*, *KCNH2*, and *KCNJ2* underlie the major repolarising ventricular potassium currents, I_{Ks} , I_{Kr} , and I_{K1} , respectively. Variations in these currents might lead to changes in the T-wave morphology is entirely consistent with the known physiology. The signal involved in both TMR^{ex} and TMR^{rec} at the *KCNQ1* locus is particularly significant as the modulation of this current by rate and sympathetic tone is one of the main mechanisms of adaptation of repolarization.³¹ Candidate genes indicated at two of the TMR^{ex} loci were *PREP* and *SOX5* from Hi-C analyses, which have also been associated with heart rate response to exercise and to recovery.³²

For TMR^{rec} , 4 of the identified loci overlapped TMR^{ex} loci (*NOS1AP*, *SCN5A-SCN10A*, *KCNQ1*, and *SOX5*). Regarding the remaining 4 loci, the variant at *KLF12* has previously been reported to be associated with the QT interval, the ST-T segment, and QRS duration. Variants at the 3 remaining loci (*CAMKD2*, *SSBP3*, and *TSC22D2*) have not been associated with an ECG marker previously. Candidate genes at these loci

include: *SSBP3*, which encodes single-stranded DNA binding protein 3, and the TMR^{rec} variant identified at this locus has been reported to be associated with P-wave parameters, with its putative function being the transcriptional regulation of the alpha 2(1) collagen gene.³³ In addition, *TSC22D2* encodes a DNA binding transcription factor. Finally, the protein *CAMK2D* regulates calcium dynamics, which is central in cardiac physiology, as the key event leading to the excitation-contraction coupling and relaxation processes.³⁴

TMR was developed based on the hypothesis that it reflects changes in the dispersion of ventricular repolarization with heart rate.⁴ Although this is the first study that attempts to investigate the biological mechanisms underlying TMR, our predictive and genetic results indicate that TMR reflects relevant electrophysiological information. Our prediction results indicate TMR is providing prognostic information independent to resting QT (reflecting total duration of ventricular repolarization) or T-wave inversions (reflecting variations in the T-wave amplitude not captured by TMR). However, genetic analyses indicate there is a substantial overlap of loci with other ECG markers, thus shared biological processes. Future studies will investigate the relation between TMR and intracardiac indices of dispersion of repolarization, which is paramount to confirm its cardiovascular predictive utility.

Cardiovascular mortality remains the most common cause of death, with >4 million victims across Europe every year.¹ Over the past 2 decades, numerous prediction models have been developed,³⁵ including the Framingham³⁶ and SCORE³⁷ models. This prediction can be further improved by including additional validated risk markers into the models. Table XVI in the [Data Supplement](#) shows the reclassification results for the addition of TMR^{rec} ≥ 0.115 to the SCORE model (Methods in the [Data Supplement](#)), indicating that TMR adds information on risk prediction beyond traditional risk factors. In addition, the significant association between the GRS for TMR^{rec} and cardiovascular events in the FULL-UKB cohort supports its potential as a cardiovascular risk predictor in high-risk populations, albeit with small HRs possibly due to the low number of events. Future work should combine ECG and genetic markers into one score (ECG markers could only be derived from EST-UKB in this study), which may show complementary cardiovascular predictive value of both TMR^{rec} and its GRS.

CONCLUSIONS

We have conducted a systematic investigation of the genetic basis of ventricular repolarization and its influence in modulating cardiovascular risk through the analysis of the T-wave morphology. We demonstrate that TMR and the GRS for TMR^{rec} are significantly associated with cardiovascular risk in a UK middle-aged population

and that TMR reflects relevant biological mechanisms influencing the risk of cardiovascular events.

ARTICLE INFORMATION

Received February 12, 2019; accepted August 20, 2019.

The Data Supplement is available at <https://www.ahajournals.org/doi/suppl/10.1161/CIRCEP.119.007549>.

Correspondence

Julia Ramirez, PhD, Clinical Pharmacology, William Harvey Research Institute, Barts and The London School of Medicine and Dentistry, Queen Mary University of London, London EC1M 6BQ, United Kingdom, Email j.ramirez@qmul.ac.uk or Patricia B. Munroe, PhD, Clinical Pharmacology, William Harvey Research Institute, Barts and The London School of Medicine and Dentistry, Queen Mary University of London, London EC1M 6BQ, United Kingdom, Email p.b.munroe@qmul.ac.uk

Affiliations

Clinical Pharmacology, William Harvey Research Institute, Barts and The London School of Medicine and Dentistry (J.R., S.v.D., A.T., M.O., P.B.M.), Centre for Advanced Cardiovascular Imaging, William Harvey Research Institute (N.A.), and National Institute of Health Research Barts Cardiovascular Biomedical Research Centre, Barts and The London School of Medicine and Dentistry (A.T., P.B.M.), Queen Mary University of London, United Kingdom. Institute of Cardiovascular Science, University College London, United Kingdom (J.R., S.v.D., P.D.L., M.O.). Barts Heart Centre, St Bartholomew's Hospital, London, United Kingdom (N.A., P.D.L.). Biomedical Signal Interpretation and Computational Simulation (BSI-CoS) group, Aragón Institute of Engineering Research, IIS Aragón, University of Zaragoza, Spain (P.L., E.P.). Biomedical Research Networking Center in Bioengineering, Biomaterials and Nanomedicine (CIBER-BBN), Spain (P.L., E.P.).

Acknowledgments

We would like to acknowledge the contribution of Alejandro Bona with the design of the graphical abstract.

Sources of Funding

This research has been conducted using the UKB Resource (application 8256) and is supported by grant MR/N025083/1 from the Medical Research Council (MRC), by the National Institutes of Health Research (NIHR) Cardiovascular Biomedical Centre at Barts and The London, Queen Mary University of London (QMUL), by the People Programme of the European Union's Seventh Framework Programme grant n° 608765 and Marie Skłodowska-Curie grant n° 786833, by the University College London Hospital Biomedicine NIHR, Barts Heart Centre Biomedical Research Centre, by grant ERC-2014-StG 638284 from the European Research Council (ERC), by project DPI2016-75458-R and by Reference Group BSICoS T39-17R cofunded by Fondo Europeo de Desarrollo Regional 2014–2020. This research utilized Queen Mary's Apocrita High-performance cluster facility, supported by QMUL Research-IT. <http://doi.org/10.5281/zenodo.438045>.

Disclosures

None.

REFERENCES

1. Townsend N, Wilson L, Bhatnagar P, Wickramasinghe K, Rayner M, Nichols M. Cardiovascular disease in Europe: epidemiological update 2016. *Eur Heart J*. 2016;37:3232–3245. doi: 10.1093/eurheartj/ehw334
2. Pak HN, Hong SJ, Hwang GS, Lee HS, Park SW, Ahn JC, Moo Ro Y, Kim YH. Spatial dispersion of action potential duration restitution kinetics is associated with induction of ventricular tachycardia/fibrillation in humans. *J Cardiovasc Electrophysiol*. 2004;15:1357–1363. doi: 10.1046/j.1540-8167.2004.03569.x
3. Nash MP, Bradley CP, Sutton PM, Clayton RH, Kallis P, Hayward MP, Paterson DJ, Taggart P. Whole heart action potential duration resti-

- tution properties in cardiac patients: a combined clinical and modeling study. *Exp Physiol.* 2006;91:339–354. doi: 10.1113/expphysiol.2005.031070
4. Ramírez J, Orini M, Mincholé A, Monasterio V, Cygankiewicz I, Luna ABd, Martínez JP, Pueyo E, Laguna P. T-wave morphology restitution predicts sudden cardiac death in patients with chronic heart failure. *J Am Heart Assoc.* 2017;6:e005310. doi:10.1161/JAHA.116.005310
 5. Ramírez J, Orini M, Mincholé A, Monasterio V, Cygankiewicz I, Bayés de Luna A, Martínez JP, Laguna P, Pueyo E. Sudden cardiac death and pump failure death prediction in chronic heart failure by combining ECG and clinical markers in an integrated risk model. *PLoS One.* 2017;12:e0186152. doi: 10.1371/journal.pone.0186152
 6. Hodkinson EC, Neijts M, Sadrieh A, Imtiaz MS, Baumert M, Subbiah RN, Hayward CS, Boomsma D, Willemsen G, Vandenberg JJ, Hill AP, De Geus E. Heritability of ECG biomarkers in the Netherlands twin registry measured from Holter ECGs. *Front Physiol.* 2016;7:154. doi: 10.3389/fphys.2016.00154
 7. Hajek C, Guo X, Yao J, Hai Y, Johnson WC, Frazier-Wood AC, Post WS, Psaty BM, Taylor KD, Rotter JL. Coronary heart disease genetic risk score predicts cardiovascular disease risk in men, not women. *Circ Genom Precis Med.* 2018;11:e002324. doi: 10.1161/CIRCGEN.118.002324
 8. Sudlow C, Gallacher J, Allen N, Beral V, Burton P, Danesh J, Downey P, Elliott P, Green J, Landray M, Liu B, Matthews P, Ong G, Pell J, Silman A, Young A, Sprosen T, Peakman T, Collins R. UK Biobank: an open access resource for identifying the causes of a wide range of complex diseases of middle and old age. *PLoS Med.* 2015;12:e1001779. doi: 10.1371/journal.pmed.1001779
 9. Orini M, Pueyo E, Laguna P, Bailon R. A time-varying nonparametric methodology for assessing changes in QT variability unrelated to heart rate variability. *IEEE Trans Biomed Eng.* 2018;65:1443–1451. doi: 10.1109/TBME.2017.2758925
 10. Srinivasan NT, Orini M, Providencia R, Simon R, Lowe M, Segal OR, Chow AW, Schilling RJ, Hunter RJ, Taggart P, Lambiase PD. Differences in the upslope of the precordial body surface ECG T wave reflect right to left dispersion of repolarization in the intact human heart. *Heart Rhythm.* 2019;16:943–951. doi: 10.1016/j.hrthm.2018.12.006
 11. Ramírez J, Orini M, Tucker JD, Pueyo E, Laguna P. Variability of ventricular repolarization dispersion quantified by time-warping the morphology of the T-Waves. *IEEE Trans Biomed Eng.* 2017;64:1619–1630. doi: 10.1109/TBME.2016.2614899
 12. Bazett HC. An analysis of the time-relations of electrocardiograms. *Ann Noninvasive Electrocardiol.* 1997;2:177–194.
 13. Malhotra A, Dhutia H, Gati S, Yeo TJ, Dores H, Bastiaenen R, Narain R, Merghani A, Finocchiaro G, Sheikh N, Steriotis A, Zaidi A, Millar L, Behr E, Tome M, Papadakis M, Sharma S. Anterior T-wave inversion in young white athletes and nonathletes: prevalence and significance. *J Am Coll Cardiol.* 2017;69:1–9. doi: 10.1016/j.jacc.2016.10.044
 14. Robin X, Turck N, Hainard A, Tiberti N, Lisacek F, Sanchez JC, Müller M. pROC: an open-source package for R and S+ to analyze and compare ROC curves. *BMC Bioinformatics.* 2011;12:77. doi: 10.1186/1471-2105-12-77
 15. Loh PR, Bhatia G, Gusev A, Finucane HK, Bulik-Sullivan BK, Pollack SJ, de Candia TR, Lee SH, Wray NR, Kendler KS, O'Donovan MC, Neale BM, Patterson N, Price AL; Schizophrenia Working Group of Psychiatric Genomics Consortium. Contrasting genetic architectures of schizophrenia and other complex diseases using fast variance-components analysis. *Nat Genet.* 2015;47:1385–1392. doi: 10.1038/ng.3431
 16. Loh PR, Tucker G, Bulik-Sullivan BK, Vilhjálmsson BJ, Finucane HK, Salem RM, Chasman DI, Ridker PM, Neale BM, Berger B, Patterson N, Price AL. Efficient bayesian mixed-model analysis increases association power in large cohorts. *Nat Genet.* 2015;47:284–290. doi: 10.1038/ng.3190
 17. Turley P, Walters RK, Maghziyan O, Okbay A, Lee JJ, Fontana MA, Nguyen-Viet TA, Wedow R, Zacher M, Furlotte NA, Magnusson P, Oskarsson S, Johannesson M, Visscher PM, Laibson D, Cesarini D, Neale BM, Benjamin DJ; 23andMe Research Team; Social Science Genetic Association Consortium. Multi-trait analysis of genome-wide association summary statistics using MTAG. *Nat Genet.* 2018;50:229–237. doi: 10.1038/s41588-017-0009-4
 18. Yang J, Lee SH, Goddard ME, Visscher PM. GCTA: a tool for genome-wide complex trait analysis. *Am J Hum Genet.* 2011;88:76–82. doi: 10.1016/j.ajhg.2010.11.011
 19. McLaren W, Gil L, Hunt SE, Riat HS, Ritchie GR, Thormann A, Flicek P, Cunningham F. The ensemble variant effect predictor. *Genome Biol.* 2016;17:122. doi: 10.1186/s13059-016-0974-4
 20. Schmitt AD, Hu M, Jung I, Xu Z, Qiu Y, Tan CL, Li Y, Lin S, Lin Y, Barr CL, Ren B. A compendium of chromatin contact maps reveals spatially active regions in the human genome. *Cell Rep.* 2016;17:2042–2059. doi: 10.1016/j.celrep.2016.10.061
 21. Staley JR, Blackshaw J, Kamat MA, Ellis S, Surendran P, Sun BB, Paul DS, Freitag D, Burgess S, Danesh J, Young R, Butterworth AS. PhenoScanner: a database of human genotype-phenotype associations. *Bioinformatics.* 2016;32:3207–3209. doi: 10.1093/bioinformatics/btw373
 22. Raudvere U, Kolberg L, Kuzmin I, Arak T, Adler P, Peterson H, Vilo J. g:Profiler: a web server for functional enrichment analysis and conversions of gene lists (2019 update). *Nucleic Acids Res.* 2019;47(W1):W191–W198. doi: 10.1093/nar/gkz369
 23. Nielsen JB, Thorolfsdottir RB, Fritsche LG, Zhou W, Skov MW, Graham SE, Herron TJ, McCarthy S, Schmidt EM, Sveinbjornsson G, Surakka I, Mathis MR, Yamazaki M, Crawford RD, Gabrielsen ME, Skogholt AH, Holmen OL, Lin M, Wolford BN, Dey R, Dalen H, Sulem P, Chung JH, Backman JD, Arnar DO, Thorsteinsdottir U, Baras A, O'Dushlaine C, Holst AG, Wen X, Hornsby W, Dewey FE, Boehnke M, Kheterpal S, Mukherjee B, Lee S, Kang HM, Holm H, Kitzman J, Shavit JA, Jalife J, Brummett CM, Teslovich TM, Carey DJ, Gudbjartsson DF, Stefansson K, Abecasis GR, Hveem K, Willer CJ. Biobank-driven genomic discovery yields new insight into atrial fibrillation biology. *Nat Genet.* 2018;50:1234–1239. doi: 10.1038/s41588-018-0171-3
 24. Bulik-Sullivan BK, Loh PR, Finucane HK, Ripke S, Yang J, Patterson N, Daly MJ, Price AL, Neale BM; Schizophrenia Working Group of the Psychiatric Genomics Consortium. LD Score regression distinguishes confounding from polygenicity in genome-wide association studies. *Nat Genet.* 2015;47:291–295. doi: 10.1038/ng.3211
 25. Lewis CM, Euesden J, O'Reilly PF. PRSice: polygenic risk score software. *Bioinformatics.* 2014;31:1466–1468. doi:10.1093/bioinformatics/btu848
 26. Kannel WB, Kannel C, Paffenbarger RS Jr, Cupples LA. Heart rate and cardiovascular mortality: the Framingham Study. *Am Heart J.* 1987;113:1489–1494. doi: 10.1016/0002-8703(87)90666-1
 27. Morshedi-Meibodi A, Larson MG, Levy D, O'Donnell CJ, Vasan RS. Heart rate recovery after treadmill exercise testing and risk of cardiovascular disease events (The Framingham Heart Study). *Am J Cardiol.* 2002;90:848–852. doi: 10.1016/s0002-9149(02)02706-6
 28. Kenttä T, Viik J, Karsikas M, Seppänen T, Nieminen T, Lehtimäki T, Nikus K, Lehtinen R, Kähönen M, Huikuri HV. Postexercise recovery of the spatial QRS/T angle as a predictor of sudden cardiac death. *Heart Rhythm.* 2012;9:1083–1089. doi: 10.1016/j.hrthm.2012.02.030
 29. Goldenberg I, Moss AJ. Long QT syndrome. *J Am Coll Cardiol.* 2008;51:2291–2300. doi: 10.1016/j.jacc.2008.02.068
 30. Roder K, Werdich AA, Li W, Liu M, Kim TY, Organ-Darling LE, Moshal KS, Hwang JM, Lu Y, Choi BR, MacRae CA, Koren G. RING finger protein RNF207, a novel regulator of cardiac excitation. *J Biol Chem.* 2014;289:33730–33740. doi: 10.1074/jbc.M114.592295
 31. Finlay M, Harmer SC, Tinker A. The control of cardiac ventricular excitability by autonomic pathways. *Pharmacol Ther.* 2017;174:97–111. doi: 10.1016/j.pharmthera.2017.02.023
 32. Ramírez J, Duijvenboden SV, Ntalla I, Mifsud B, Warren HR, Tzani E, Orini M, Tinker A, Lambiase PD, Munroe PB. Thirty loci identified for heart rate response to exercise and recovery implicate autonomic nervous system. *Nat Commun.* 2018;9:1947. doi: 10.1038/s41467-018-04148-1
 33. Bayarsaihan D, Soto RJ, Lukens LN. Cloning and characterization of a novel sequence-specific single-stranded-DNA-binding protein. *Biochem J.* 1998;331(pt 2):447–452. doi: 10.1042/bj3310447
 34. Mattiazzi A, Bassani RA, Escobar AL, Palomeque J, Valverde CA, Vila Petroff M, Bers DM. Chasing cardiac physiology and pathology down the CaMKII cascade. *Am J Physiol Heart Circ Physiol.* 2015;308:H1177–H1191. doi: 10.1152/ajpheart.00007.2015
 35. Damen JA, Hooft L, Schuit E, Debray TP, Collins GS, Tzoulaki I, Lassale CM, Siontis GC, Chiochia V, Roberts C, Schlüssel MM, Gerry S, Black JA, Heus P, van der Schouw YT, Peelen LM, Moons KG. Prediction models for cardiovascular disease risk in the general population: systematic review. *BMJ.* 2016;353:i2416. doi: 10.1136/bmj.i2416
 36. Anderson KM, Odell PM, Wilson PW, Kannel WB. Cardiovascular disease risk profiles. *Am Heart J.* 1991;121(1 pt 2):293–298. doi: 10.1016/0002-8703(91)90861-b
 37. Conroy RM, Pyörälä K, Fitzgerald AP, Sans S, Menotti A, De Backer G, De Bacquer D, Ducimetière P, Jousilahti P, Keil U, Njølstad I, Oganov RG, Thomsen T, Tunstall-Pedoe H, Tverdal A, Wedel H, Whincup P, Wilhelmsen L, Graham IM; SCORE project group. Estimation of ten-year risk of fatal cardiovascular disease in Europe: the SCORE project. *Eur Heart J.* 2003;24:987–1003. doi: 10.1016/s0195-668x(03)00114-3